Design and test of one-rotor orchard horizontal rotary rake based on tine movement trajectory analysis

Xiaohui Lei[1], Xiaolan Lyu[1*], Yongzhe Shen[2], Shicheng Qian[3], Jin Zeng[1], Quanchun Yuan[1], Yannan Qi[1], Wanxi Huang[1], Zhengbao Ma[3]

(1. *Institute of Agricultural Facilities and Equipment, Jiangsu Academy of Agricultural Sciences/ Key Laboratory of Modern Horticultural Equipment, Ministry of Agriculture and Rural Affairs, Nanjing 210014, China*;
2. *Liaoning Agricultural Mechanization Development Center, Shenyang 110034, China*;
3. *Jiangsu Agricultural Machinery Development and Application Center, Nanjing 210017, China*)

Abstract: To solve the problem of effective utilization of orchard green fertilizer, a small one-rotor orchard horizontal rotary rake (OHRR) was developed, which is used for grass collection in the mowing agronomic section of orchard management. In the working process, the disc drives the arms rotating around the vertical shaft, the guide cam that is fixed to the vertical shaft controls tine movement, and the tines turn to different inclination angles in different positions. The kinematic validation model of OHRR was built based on the theory that there is no gap or small overlap between the two adjacent working areas of the tines. This model determines the relationship between the advancing speed, disc rotational speed, rotation radius, arm number, and tine working width. The leakage and repeating rate of OHRR virtual prototype were calculated by tines movement trajectories analysis in multi-body dynamics simulation. Box-Behnken three-factor and three-level test plans for advancing speed, disc rotational speed, and tine working width were designed to obtain the optimal operation parameters of the OHRR: advancing speed was 11.16 km/h, disc rotational speed was 6.98 rad/s, and tines working width was 0.3 m. Taking labor working as the control group, OHRR field tests were evaluated by four indices: strip density, leakage rate, working efficiency, and profitable area. Field tests results showed that the leakage rate of OHRR was 4.56%, which meets the requirements of national standard JB/T10905. The strip density, width, and height of OHRR were 29.44 kg/m^3, 0.5 m, and 0.25 m, respectively. These data can provide support for the subsequent loading and transportation operation. The profitable area of OHRR was 6.7 hm^2, which is suitable for large-scale mechanized orchard management.

Keywords: orchard, rake, tine movement model, performance parameter, trajectory optimization
DOI: 10.25165/j.ijabe.20251802.9194

Citation: Lei X H, Lyu X L, Shen Y Z, Qian S C, Zeng J, Yuan Q C, et al. Design and test of one-rotor orchard horizontal rotary rake based on tine movement trajectory analysis. Int J Agric & Biol Eng, 2025; 18(2): 115–123.

1 Introduction

Fruit is the third largest agricultural product in China, covering an area of approximately 12 666 730 hm^2, with an annual output exceeding 300 million t and an annual value of about 192.93 billion US dollars. More than 100 million farmers in China are engaged in fruit production, playing a significant role in the agricultural economy. Currently, the fruit production industry in China is facing challenges such as labor shortages, low levels of mechanization rates (less than 30%), and low production efficiency. There is an urgent need to develop new-quality productivity to empower the transformation and upgrading of the fruit industry. Planting grass is a modern orchard management method of planting pasture as mulch throughout the orchard[1,2]. It can improve soil physical and chemical properties, raise soil water storage, and enhance orchard tree disease resistance[3-5]. Overgrown grass will compete with fruit trees for soil nutrients, which need to be mowed four to five times per year[6,7]. At present, the common treatment method of mowed stems in China is to spread them on the orchard ground directly for fertilizer[8]. Compared with centralized fertilizer management, this treatment method not only affects the growth of orchard grass, but also has poor fertilizer efficiency. Labor working is time-consuming and low efficiency, and natural fertilizer has poor effect. Thus it is urgent to develop orchard raking machinery.

The rake is a kind of tractor traction harvest machine, which collects the mowed pasture on the ground. The application of the rake concentrated in the pasture, and all of them are large models. It can be divided into horizontal rotary type, finger disc type, and fence type. Research and development on the rake in China are concentrated in the Inner Mongolia region[9,10]. Liu et al.[11] developed a double rotor horizontal rotating rake, whose leakage rate was 2%, working width was 5 m, and working efficiency was 4.1 hm^2/h. Compared with labor, it can increase labor productivity by 38 times and reduce operation cost by 40%. Wang et al.[12] analyzed the loading characteristics of the 9LSQ-5.3 type double-rotor horizontal rotatory rake, optimally selected 55Si2Mn as tine material and tine

Received date: 2024-07-02 **Accepted date:** 2025-03-10
Biographies: Xiaohui Lei, Research Associate, research interest: orchard management machinery, Email: leixiaohui.2008@163.com; **Yongzhe Shen**, Senior Agronomist, research interest: orchard management machinery, Email: shenyongzhe1988@126.com; **Shicheng Qian**, Engineer, research interest: orchard management machinery, Email: qsc2824@163.com; **Jin Zeng**, Research Assistant, research interest: orchard management machinery, Email: j-zeng@jaas.ac.cn; **Quanchun Yuan**, Research Assistant, research interest: orchard management machinery and its application, Email: yuanquanchun@jaas.ac.cn; **Yannan Qi**, Research Assistant, research interest: orchard management machinery, Email: qiyn1020@163.com; **Wanxi Huang**, Engineer, research interest: orchard management machinery, Email: 597774265@qq.com; **Zhengbao Ma**, Researcher, research interest: orchard management machinery, Email: 13851780516@163.com.

***Corresponding author: Xiaolan Lyu**, Researcher, research interest: orchard management machinery. Institute of Agricultural Facilities and Equipment, Nanjing 210014, China. Email: lxlanny@126.com.

fatigue life was increased from 4955 to 8374 h. Zhai et al.[13], based on TRIZ theory, proposed an improved scheme for the ground profile mechanism of double-rotor horizontal rotary, which solved the problem of poor profile performance. The relevant studies in China are mostly about the structure design of parts and components, such as spring tine, profile mechanism, gear box, and so on. The mathematical calculation methods in the references now can only verify whether the structural parameters meet the operation requirements of the machine. The optimization of performance parameters is not reported, and the rake has not been applied in the field of orchard mechanized management. Mainstream rakes are manufactured by international agricultural machinery companies and their types are various, such as the LINER series made by CLAAS in Germany, GA series made by KUHN in France, and WR series made by John Deere in America[14]. These machines are mainly used for forage harvesting, and there are no reports on orchard raking machines. Paraforos et al.[15] presented a methodology to predict accumulated fatigue damage of rake. The differences between the accumulated fatigue damage predicted from the simulations and from the measured data had mean value and standard deviation equal to −22% and 12.8%, respectively. Abby et al.[16] researched the effect of rake on ash content and forage nutritive values of alfalfa. The results show that using a hay merger or sidebar rake to combine swaths resulted in less ash content compared with a wheel rake; however, rake type rarely resulted in differences in forage nutritive values. Khalid investigated the impact of different patterns of raking and baling operations on the dry matter and quality losses of the produced alfalfa hay[17]. The best result was baling-III, for which dry matter losses were 2.01% of the total hay yield and the crude protein losses were 1.44% of the total crude protein. As the market products of foreign rakes have matured, the relevant research is no longer on the structural design of the machine, but focuses more on performance evaluation, such as fatigue damage, ash content, forage nutritive values, dry matter, and quality losses. This research can provide reference for the future development of the orchard rake.

The height of the horizontal rotary rake is lower than other types of rakes, suitable for the characteristics of modern orchard dwarfing and high-density planting. Combined with the tines movement trajectory optimization and field tests, this study develops a small one-rotor orchard horizontal rotary rake (OHRR), which is used for grass collection in the mowing agronomic section of orchard management. The goal of optimization is reducing the repeating rate, with the premise of ensuring the leakage rate meets the national standard[18]. Three performance parameters were optimized by Box-Behnken design: advancing speed, disc rotational speed, and tine working width of the rake. This paper can provide reference for the development of the orchard rake.

2 Materials and methods

2.1 Machine structure and working principle

OHRR is linked with a tractor by three-point suspension. The whole machine is composed of a body frame, a transmission mechanism, a cam guide mechanism, arms, spring tines, and a limit wheel. The structure of the OHRR is shown in Figure 1. The whole work process of the machine is completed by the hydraulic control system and mechanical transmission system of the tractor, and the rake power shaft is connected with the tractor power take off (PTO) by the universal shaft. The tractor hydraulic system adjusts the operating height of the rake, and PTO provides power to the disc for rotation. Most of the modern orchards in China are dwarf and high-density planted, with a row spacing range of 4 to 5 m[19,20]. Considering the cultivation method of putting grass cloth around young fruit trees, as well as the characteristics of ridge cultivation, the working width of the machine is set to 3 m[21,22]. The pasture horizontal rotor rakes that have been made mainly consist of two to four rotors and six to twelve arms. Considering the machine manufacturing cost and the working condition, the arm number of the machine in this study is set to six. The main structure and performance parameters of OHRR are listed in Table 1.

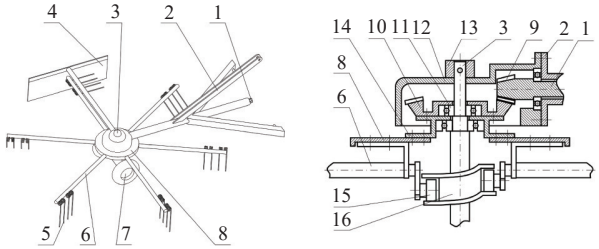

a. External structure b. Internal structure

1. Power shaft 2. Rack 3. Vertical shaft 4. Grass block 5. Spring tine 6. Arm 7. Limit wheel 8. Disc 9. Power shaft bevel gear 10. Bevel gear wheel 11. Bear 12. Bear box shell 13. Vertical shaft fixed block 14. Connection bolt 15. Arm pulley 16. Guide cam

Figure 1 Structure of the rake

Table 1 Main structural and performance parameters

Name	Value
Tractor minimium power/kW	18.8
Mass/kg	200
Size (length×width×height)/m×m×m	3.50×3.00×0.95
Working width/m	3
Advancing speed/(km·h^{-1})	11.16
PTO rotational speed/(r·min^{-1})	540
Arm number	6
Tine working width/m	0.3
Leakage rate/%	4.38
Strip density/(km·m^{-3})	29.44
Strip size (width×height)/m×m	0.5×0.25
Working efficiency/(hm^2·h^{-1})	3.35
Profitable area/hm^2	6.7

When OHRR is working, the tractor adjusts the machine to a suitable operating height by hydraulic lifting, then the PTO drives the disc to rotate, and finally the tractor drives the rake forward. PTO transfers energy through the universal shaft to the rake power shaft. The bevel gear at the end of the rake power shaft transfers the energy to the large bevel gear which is fixed to the disc. The disc drives the arms to rotate around the vertical shaft, and the guide cam that is fixed to the vertical shaft controls tine movement. The guide cam is embedded around the vertical shaft in the form of a track wall, and the arm pulley is connected to the guide cam track in the form of a sliding pair, controlling the arm according to the changes in the track curve trajectory, and the tines turn to different inclination angles in different positions. The collection action of grass cut off stems is completed by the interaction between tines and the grass block. The limit wheel is used to prevent the bottom of the tines from touching the ground and to ensure the high working quality. The working process of the tines is shown in Figure 2. OHRR moves along the *Y*-axis, the disc rotates counter clockwise, and the negative direction of the *X*-axis is the direction of grass block. During the rotation of the disc: point 1 to point 2, the direction of tines is parallel to the ground; point 2 to point 3, the

directions between tines and the ground are gradually changed from parallel to vertical; point 3 to point 4, the direction of tines is vertical to the ground; point 4 to point 5, the directions between the tines and the ground are gradually changed from vertical to parallel; point 5 to point 1, the direction of tines is parallel to the ground. Designed θ_1=20°, θ_2=70°, θ_3=70°, θ_4=20°.

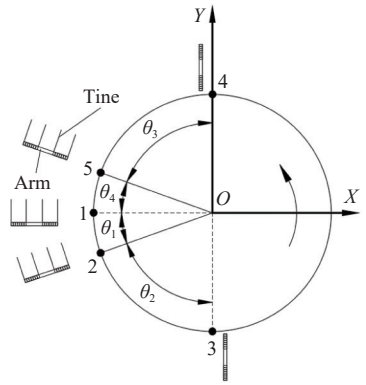

Figure 2 Working process of tines

Taking the center point of the disc as O, the horizontal direction to the right is the positive direction of the X-axis, and the vertical direction forward is the positive direction of the Y-axis, to form a rectangular plane coordinate system, as shown in Figure 3. The leakage area is the uncrossed area of the tine work, while the repeating area is the area of the tine work which is crossed two or more times. Leakage rate in Figure 3 is defined as the ratio of leakage area to working area in one cycle of disc rotation; repeating rate in Figure 3 is the ratio of repeating area to working area in one cycle of disc rotation, as shown in Equations (1) and (2).

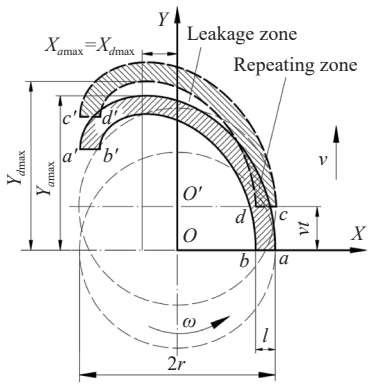

Note: O and O' are the center points of the disc before and after movement; a, b are the outermost and innermost points of tine work on the first arm; c, d are the outermost and innermost points of tine work on the second arm; The thick solid line area ($aa'b'b$) and dashed line area ($cc'd'd$) indicate the trajectories of the tines of the first and second arm; Coordinate values X_{amax} and Y_{amax} indicate the highest point of curve aa'; coordinate values X_{dmax} and Y_{dmax} indicate the highest point of curve dd'; v is the advancing speed of OHRR, m/s; t is working time, s; ω is disc rotational speed, rad/s; r is rotation radius of the OHRR, m; l is tine working width, m.

Figure 3 Trajectory of tine movement

$$E_l = \frac{A_l}{A} \times 100\% \tag{1}$$

where, E_l is leakage rate, %; A_l is the leakage area in one disc rotation cycle, m^2; A is the driving area of OHRR in one disc rotation cycle, m^2.

$$E_r = \frac{A_r}{A} \times 100\% \tag{2}$$

where, E_r is repeating rate, %; A_r is the repeating area in one disc rotation cycle, m^2.

The movement equation of point a is:

$$\begin{cases} X_a = r\cos\omega t \\ Y_a = r\sin\omega t + vt \end{cases} \tag{3}$$

where, X_a is the value of point a on X-axis, m; Y_a is the value of point a on Y-axis, m; r is the rotation radius of OHRR, m; ω is the disc rotational speed, rad/s; t is working time, s; v is the advancing speed of OHRR, m/s.

The movement equation of point d is:

$$\begin{cases} X_d = (r-l)\cos\left(\omega t - \dfrac{2\pi}{n}\right) \\ Y_d = (r-l)\sin\left(\omega t - \dfrac{2\pi}{n}\right) + vt \end{cases} \tag{4}$$

where, X_d is the value of the point d on X-axis, m; Y_d is the value of the point d on Y-axis, m; l is the tine working width, m; n is arm number.

Take the maximum values of point a and point d on Y-axis by taking the derivatives of Y_a and Y_d in Equations (3) and (4), that is:

$$Y_{a\max} = \frac{v}{\omega}\arccos\left(-\frac{v}{\omega r}\right) + r\sin\left[\arccos\left(-\frac{v}{\omega r}\right)\right] \tag{5}$$

$$Y_{d\max} = v\left[\frac{2\pi}{\omega n} + \frac{1}{\omega}\arccos\left(-\frac{v}{\omega(r-l)}\right)\right] + (r-l)\sin\left[\arccos\left(-\frac{v}{\omega(r-l)}\right)\right] \tag{6}$$

where, Y_{amax} is the maximum value of the point a on Y-axis, m; Y_{dmax} is the maximum value of the point d on Y-axis, m.

To reduce the leakage rate, Y_{amax} should be greater than Y_{dmax}, which means

$$Y_{a\max} \geq Y_{d\max} \tag{7}$$

Substitute Equations (5) and (6) into Equation (7), and Equation (8) is obtained. This is the kinematic model of OHRR and determines the relationship between the advancing speed, disc rotational speed, rotation radius, arm number, and tine working width. However, Equation (8) can only be used as a validation model, not an optimization model.

$$\frac{2\pi v}{n\omega r} = \sqrt{1-\frac{v^2}{\omega^2 r^2}} - \sqrt{\left(1-\frac{l}{r}\right)^2 - \frac{v^2}{\omega^2 r^2}} - \frac{v}{\omega r}\arccos\left[\frac{r}{r-l}\left(\frac{v^2}{\omega^2 r^2} + \sqrt{1+\frac{v^2}{\omega^2 r^2}}\right)\sqrt{\left(1-\frac{l}{r}\right)^2 - \frac{v^2}{\omega^2 r^2}}\right] \tag{8}$$

2.2 Methods of tests

To get tine movement trajectories, the virtual working process of OHRR was analyzed based on ADAMS software[23-26]. According to the size parameters of the OHRR, the mechanical drawing software PTC/Creo was used to draw the 3D prototype assembly drawing, which was stored in Parasolid format exported to ADAMS. In ADAMS, the kinematics constraint relation was added to the constraint library, and the driver was added to the driver library. The rotating motion between the rack and the disc was realized by adding the rotating pair and the rotating drive to simulate the rotation of the disc. The displacement between the rack and ground was realized by adding the slip pair and the slip drive to simulate the moving of the machine. Two marker points were added to the bottom of tines that outermost and innermost of the arm, which to draw the tines movement trajectories. Six arms were

marked with a total of twelve marker points, from Marker 1 to Marker 12. The trajectory of virtual prototype simulation is shown in Figure 4. The six color trajectories of red, black, green, purple, blue, and cyan are the outermost and innermost points of the tines of each arm, respectively.

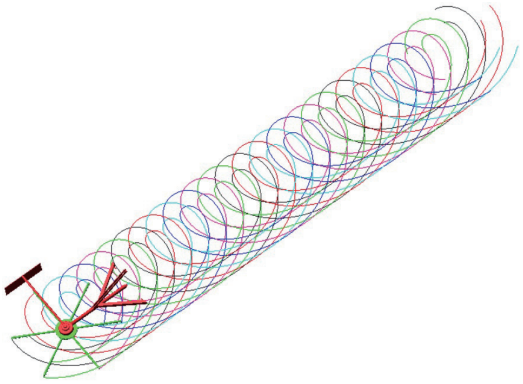

Figure 4 Trajectory of virtual prototype simulation

According to Box-Behnken central combination theory, taking leakage and repeating rate as the response values, three-factor and three-level test plans for advancing speed, disc rotational speed, and tine working width are designed in Design-Expert software[27, 28]. Referring to the national standard JB/T10905[18], the range of advancing speed is set from 6 to 12 km/h. For disc rotational speed, when the linear velocity of the outermost point of the arm is lower than 6 m/s, the ability of mowed stems interaction decreases, but when the linear velocity is higher than 12 m/s, the raking effect is not good under the impact of tines on mowed stems[29]. Since the rotation radius of the OHRR was 1.5 m, according to the rotational angular velocity formula, the range of disc rotational speed was set from 4 to 8 rad/s. In the market, the width of one single tine is 0.1 m, and the number of tines on rake arm is from one to three. The range of tine working width is set from 0.1 to 0.5 m. Factors and levels of the test are listed in Table 2.

Table 2 Factors and levels of test

Levels	Advancing speed/(km·h^{-1})	Disc rotational speed/(rad·s^{-1})	Tine working width/m
−1	6.00	4.00	0.10
0	9.00	6.00	0.30
1	12.00	8.00	0.50

Referring to Chinese standard JB/T9700[30] and GB/T14247[31], field tests were carried out in the breeding orchard of Jiangsu Academy of Agricultural Sciences in September 2024. The operating parameters of OHRR were carried out according to the optimal results of Box-Behnken test. The test site is shown in Figure 5. Taking labor working as the control group, OHRR field tests were evaluated by four indices: strip density, leakage rate, working efficiency, and profitable area[32]. OHRR group test was repeated five times. In each test, five section grass strips (1 m long) were randomly selected to detect the grass strips' density, and 1 m^2 square block of working zone of each sample grass strip was selected to detect the leakage rate. Measurement point distribution is shown in Figure 6. For the control group, five operators were employed and each of them randomly selected five square plots (each point 1 m^2) to collect grass. The ranges of measurement points are calibrated using self-made 1 m×1 m square wooden frames, and the main measuring instruments include steel rulers, electronic balances (with a precision of 0.01 g), and calculators (accurate to two decimal places). The cross section of grass strip is approximately triangular in shape, so the cross section area calculation is made assuming the shape of a triangle. Three cross sections of each grass strip were randomly selected to measure its bottom length and height, and the average area was taken as the cross section area of the grass strip. The cross section area and strip density were calculated according to Equations (9) and (10), respectively. To reflect the stability of strip density, the average strip density, standard deviation, and coefficient of variation were calculated, as shown in Equations (11) to (13). Referring to the national standard GB/T14247[31], the leakage weight was defined as the grass stem with the length greater than 7 cm after raking. The leakage rate of OHRR and labor group was calculated according to Equations (14) and (15), respectively. The calculation method of coefficient of variation of strip width, strip height, and leakage rate were the same as that of strip density.

Figure 5 Field test site

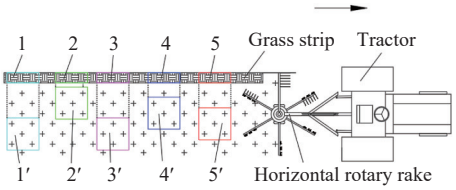

Note: Arrow is the working direction of OHRR, 1 to 5 are strip sample numbers, and 1′ to 5′ are sample numbers of leakage rate measurement.

Figure 6 Measurement point distribution

$$A_{ic} = \frac{1}{6}(l_{ic1}h_{ic1} + l_{ic2}h_{ic2} + l_{ic3}h_{ic3}) \tag{9}$$

where, A_{ic} is the cross section area of sample i, m^2; l_{ic1} is the bottom length of cross section 1 of sample i, m; h_{ic1} is the height of cross section 1 of sample i, m; l_{ic2} is the bottom length of cross section 2 of sample i, m; h_{ic2} is the height of cross section 2 of sample i, m; l_{ic3} is the bottom length of cross section 3 of sample i, m; h_{ic3} is the height of cross section 3 of sample i, m.

$$\rho_i = \frac{m_{is}}{A_{ic}} \tag{10}$$

where, ρ_i is the strip density of sample i, kg/m^3; m_{is} is the strip weight of sample i, kg.

$$\rho = \frac{\sum_{i=1}^{5}\rho_i}{5} \tag{11}$$

where, ρ is the average strip density, kg/m^3.

$$S_\rho = \sqrt{\frac{\sum_{i=1}^{5}(\rho_i - \rho)^2}{5}} \tag{12}$$

where, S_ρ is the standard deviation of the strip density, kg/m^3.

$$\mathrm{CV}=\frac{S_\rho}{\rho}\times 100\% \tag{13}$$

where, CV is the coefficient of variation of the strip density, %.

$$E_{Ml}=\frac{3m_{Ml}}{m_s}\times 100\% \tag{14}$$

where, E_{Ml} is leakage rate of OHRR, %; m_{Ml} is leakage weight of OHRR, kg.

$$E_{Ll}=\frac{3m_{Ll}}{m_{Ls}}\times 100\% \tag{15}$$

where, E_{Ll} is leakage rate of labor, %; m_{Ll} is leakage weight of labor, kg; m_{Ls} is collection weight of labor, kg.

The working time of two groups were recorded and converted to working efficiency. The profitable area of OHRR was calculated based on the working efficiency, so as to guide the orchard manager to make a decision. The profitable area of the machine is the minimum planting area required by the machine to replace labor in management cost. According to Equations (16)-(18), the profitable area can be calculated. When the planting area of crops is larger than the profitable area, the machine can bring about profits.

$$q=\frac{p}{n_y} \tag{16}$$

where, q is the annual depreciation of OHRR, \$; p is the price of OHRR, \$; n_y is the depreciable life, years.

$$c=\frac{c_0 t}{t_0}\times\eta \tag{17}$$

where, c is the cost that can be saved by the rake by replacing labor, \$/hm^2; c_0 is the labor cost in an 8 h working day, \$; t is the average labor working time per unit area, h/hm^2; t_0 is the working hours (8 h) in one day, h; η is the proportion of time saved by machine compared to labor.

$$A=\frac{q+c_{uml}}{c} \tag{18}$$

where, A is profitable area of OHRR, hm^2; c_{uml} is the cost of use, maintenance, and labor operation of tractor for OHRR per year, \$.

3 Results and discussion

3.1 Simulation test

Since ADAMS does not have the function of calculating the zone area, the points coordinate data were exported by ADAMS and drawn in the form of a spline curve in mechanical drawing software AutoCAD after being uniformly corrected by the global coordinates. In AutoCAD, tine movement trajectory of one disc rotation cycle was taken out by the breakpoint command, while the leakage area and repeating area were calculated by the area command. Box-Behnken test response values are listed in Table 3, and tine movement trajectories of one disc rotation cycle in Box-Behnken test are shown in Figure 7.

Quadratic regression fitting analysis was conducted on the results of Table 3 using Design-Expert software, and the regression equations of leakage rate and repeating rate were built, as shown in Equations (19) and (20):

$$E_l=2.1+8.95X_1-9.12X_2-23.75X_3-6.66X_1X_2-9.12X_1X_3+7.42X_2X_3+4.09X_1^2+4.83X_2^2+18.23X_3^2 \tag{19}$$

where, E_l is leakage rate, %; X_1 is the level of advancing speed; X_2 is the level of disc rotational speed; X_3 is the level of tine working width.

$$E_r=69.24-17.16X_1+13.61X_2+33.42X_3+6.17X_1X_2+1.6X_1X_3+3.42X_2X_3+1.71X_1^2-3.57X_2^2-15.5X_3^2 \tag{20}$$

where, E_r is repeating rate, %.

Table 3 Test design and response values

No.	Level of advancing speed	Level of disc rotational speed	Level of tine working width	Leakage rate/%	Repeating rate/%
1	0	−1	−1	65.02	8.66
2	1	−1	0	35.36	22.95
3	0	0	0	2.21	65.24
4	0	0	0	1.66	75.24
5	1	1	0	3.68	67.18
6	−1	−1	0	5.05	79.91
7	0	0	0	2.15	73.24
8	−1	0	1	0	99.03
9	0	0	0	2.65	68.24
10	0	1	1	0.15	98.52
11	0	−1	1	3.43	69.14
12	−1	1	0	0	99.47
13	0	0	0	1.84	64.24
14	1	0	1	0.58	78.22
15	0	1	−1	32.05	24.36
16	1	0	−1	67.07	8.68
17	−1	0	−1	30.02	35.87

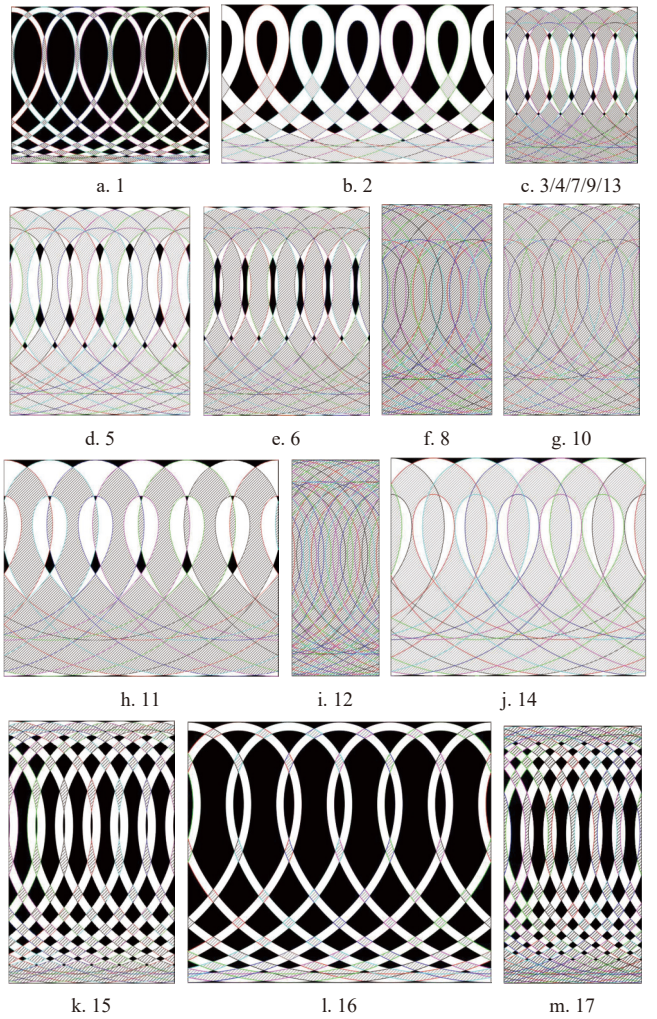

Note: The prototype runs from left to right and the disc rotates counterclockwise, the black zone is the leakage zone, and the shaded zone is the repeating zone.

Figure 7 Tine movement trajectory of Box-Behnken test

Variance analysis results are listed in Table 4. For the regression model $p<0.0001$, while for lack of fit $p>0.05$, indicating a significant regression model and non-significant lack of fit. This reflects the relationship between the advancing speed, disc rotational speed, and tine working width with leakage and repeating rates. The determination coefficient R^2 of the model is 0.9996 for leakage rate and 0.9757 for repeating rate, meaning the two models can explain 97% of the change in their response values. The test errors of the two models are small, thus showing that the models can be used to analyze and predict the leakage and repeating rates.

Table 4 Variance analysis results

Index	Sources	Sum of squares	*df*	Mean square	*F*	*p*
E_l	Model	8212.30	9	912.48	1876.79	< 0.0001
	X_1	641.18	1	641.18	1318.78	< 0.0001
	X_2	665.76	1	665.76	1369.34	< 0.0001
	X_3	4512.50	1	4512.50	9281.35	< 0.0001
	X_1X_2	177.29	1	177.29	364.65	< 0.0001
	X_1X_3	332.52	1	332.52	683.92	< 0.0001
	X_2X_3	220.37	1	220.37	453.27	< 0.0001
	X_1^2	70.36	1	70.36	144.71	< 0.0001
	X_2^2	98.34	1	98.34	202.26	< 0.0001
	X_3^2	1398.95	1	1398.95	2877.38	< 0.0001
	Residual	3.40	7	0.49		
	Lack of fit	2.83	3	0.94	6.51	0.0510
	Pure error	0.58	4	0.14		
	Correction total	8215.70	16			
E_r	Model	14 073.69	9	1563.74	31.19	< 0.0001
	X_1	2354.70	1	2354.70	46.97	0.0002
	X_2	1481.58	1	1481.58	29.55	0.0010
	X_3	8933.83	1	8933.83	178.21	< 0.0001
	X_1X_2	152.15	1	152.15	3.04	0.1250
	X_1X_3	10.18	1	10.18	0.20	0.6659
	X_2X_3	46.79	1	46.79	0.93	0.3662
	X_1^2	12.29	1	12.29	0.25	0.6356
	X_2^2	53.70	1	53.70	1.07	0.3351
	X_3^2	1011.42	1	1011.42	20.18	0.0028
	Residual	350.92	7	50.13		
	Lack of fit	256.92	3	85.64	3.64	0.1218
	Pure error	94.00	4	23.50		
	Correction total	14 424.61	16			

The effects of the interactive factors of advancing speed, disc rotational speed, and tine working width on leakage and repeating rates are shown in Figure 8. Figure 8a shows the effect of advancing speed and disc rotational speed on the leakage and repeating rates when the tine working width is located at the center level (0.3 m); reducing advancing speed and increasing disc rotational speed can reduce the leakage rate and increase the repeating rate. Figure 8b shows the effect of advancing speed and tine working width on the leakage and repeating rates when the disc rotational speed is located at the center level (6 rad/s); reducing advancing speed and increasing tine working width can reduce the leakage rate and increase the repeating rate. Figure 8c shows the effect of disc rotational speed and tine working width on the leakage and repeating rates when the advancing speed is located at the center level (9 km/h); increasing disc rotational speed and tine working width can reduce the leakage rate and increase the repeating rate. The leakage rate is positively related to the advancing speed and is inversely related to the disc rotational speed and tine working width, while the repeating rate is inversely related to the advancing speed and is positively related to the disc rotational speed and tine working width.

The influence of each parameter on regression equation is reflected by *p*-value. $p<0.01$ indicates an extremely significant influence of parameter's on the model, and $p<0.05$ indicates a significant influence on the model. All regression terms influence the leakage rate extremely significantly; Equation (19) is already the optimal model. Regression terms X_1, X_2, X_3, and X_3^2 influence the repeating rate extremely significantly, while the other regression terms are not significant. Optimization Equation (21) is obtained after the repeating rate removes the insignificant regression terms. The *p*-value of the optimized repeating rate model is less than 0.001, and the *p*-value of the lack of fit is more than 0.05, indicating that the optimized model is reliable. Taking the range of 0 to 5% as the limiting condition of the leakage rate, and aiming at minimizing the repeating rate, the parameters of advancing speed, disc rotational speed, and tine working width were optimized in Design-Expert software. The optimal operation parameters of the OHRR were obtained as follows: advancing speed was 11.16 km/h, disc rotational speed was 6.98 rad/s, and tine working width was 0.3 m. Correspondingly, the leakage rate was 5%, and the repeating rate was 62.74%.

$$E_r = 68.41 - 17.16X_1 + 13.61X_2 + 33.42X_3 - 15.6X_3^2 \quad (21)$$

3.2 Field test

The purpose of the rake is to collect grass into a strip for subsequent loading and transportation. Leakage rate and strip density are two important indices to evaluate the working quality. Leakage rate and its coefficient of variation of two groups are listed in Table 5, and leakage and collection weight of two groups are shown in Figure 9. The average leakage rate of OHRR is 4.56%, showing a small discrepancy with the simulation results. One reason for the discrepancy is that the tractor was operated by the driver, so the advancing speed will fluctuate within a small range. Another reason is that in the actual operation process of OHRR, not only are the tines acting on the grass stems, but also the grass stems interact with each other. The grass stem in the leakage zone will be driven by the grass stem in the operation zone. Moreover, the average leakage rate of OHRR is less than 5%, which meets the requirements of national standard JB/T10905[18]. The average leakage rate of labor group is 9.35%, which is almost two times that of OHRR. The reason can be seen from Figure 9, where the average collection weight of the two groups is 0.61 kg for OHRR and 0.59 kg for labor, and the average leakage weight of the two groups is 0.03 kg for OHRR and 0.06 kg for labor. The large difference between the molecules leads to different results; the leakage weight of labor is much larger than that of OHRR in the same area range. The artificial collection method is to grasp the grass by labor, and the leakage weight is controlled by the operator in a subjective manner. Therefore, the fatigue caused by a long time of operation will greatly affect the weight. The coefficient of variation of the labor group is larger than that of OHRR. It can be seen intuitively from Figure 9that the data fluctuation of the labor group is larger than that of OHRR. The distribution of grass varies between orchard rows, with some sample points flourishing and others sparse. Collection weight of OHRR was calculated from strip weight and is the average value of 3 m^2 area, but collection weight of the labor group is only from 1 m^2 area. In addition, the tractor of OHRR follows a fixed route and is more stable than labor operation. The leakage weight fluctuation of labor is larger than that of OHRR.

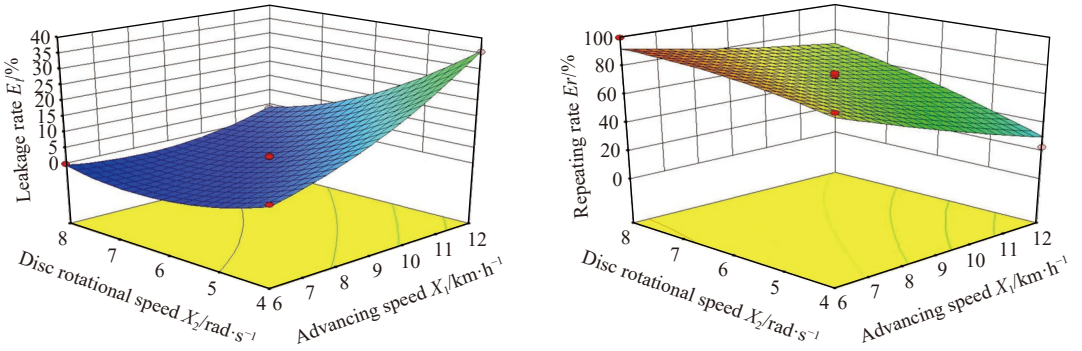

a. Effects of X_1X_2 on E_l and E_r when X_3 is 0.3 m

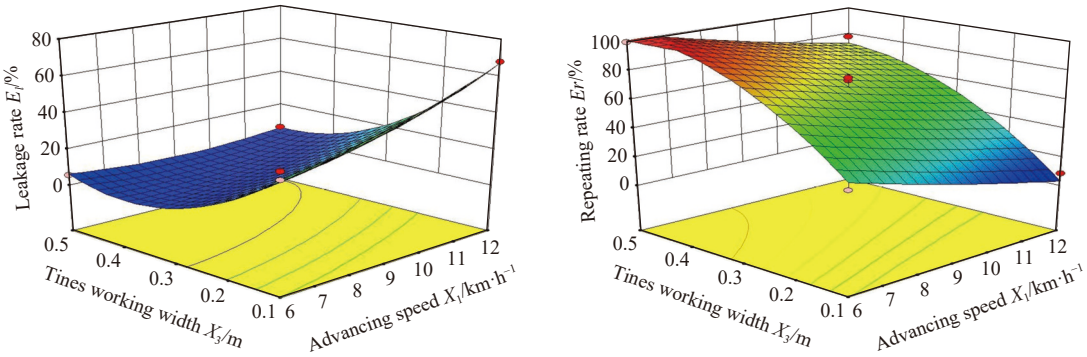

b. Effects of X_1X_3 on E_l and E_r when X_2 is 6 rad/s

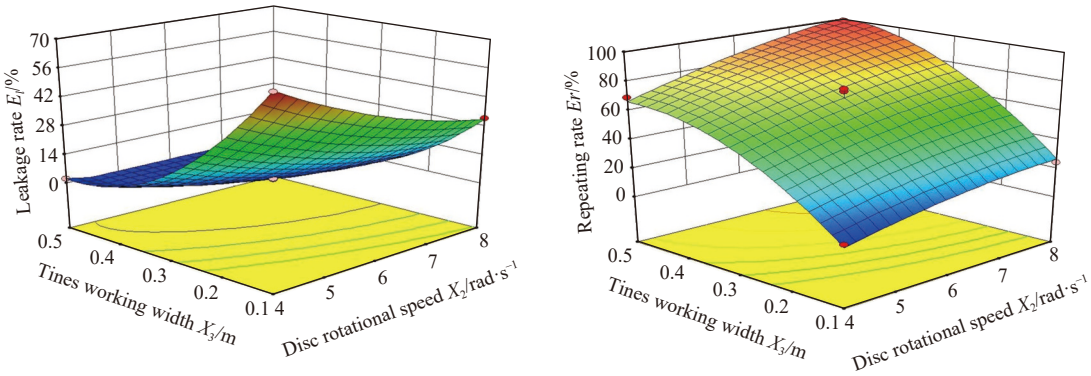

c. Effects of X_2X_3 on E_l and E_r when X_1 is 9 km/h

Figure 8 Effects of interactive factors of advancing speed, disc rotational speed, and tine working width on leakage and repeating rates

Table 5 Leakage rate and coefficient of variation (CV)

Test number	Index	OHRR	Labor
1	Leakage rate/%	4.61	9.31
	CV/%	4.95	12.38
2	Leakage rate/%	4.51	9.61
	CV/%	4.34	12.27
3	Leakage rate/%	4.84	9.45
	CV/%	4.12	11.63
4	Leakage rate/%	4.50	9.28
	CV/%	4.38	11.75
5	Leakage rate/%	4.36	9.09
	CV/%	4.41	12.59
Average leakage rate/%		4.38	9.35
Average CV/%		4.43	12.12

Strip density, width, height, and its coefficient of variation are listed in Table 6. The average strip density, width, and height are 29.44 kg/m^3, 0.5 m, and 0.25 m, respectively. These data can provide support for the subsequent loading and transportation operation. The average coefficients of variation of these three parameters are 5.16%, 5.26%, and 5.27%, respectively. They reflect small data fluctuation and better grass strip. The strip width is 0.5 m, which is inconsistent with the tine working width of 0.3 m, because the strip width is jointly determined by the tine working width and the grass block. The working efficiency of the two groups is tested and the results are listed in Table 7. The working efficiency of OHRR is much higher than that of labor, at 30 times higher. The price of OHRR is $413.35, with five years of depreciable life. The orchard are raked 4 or 5 times per year, and the use, maintenance, and labor operation costs of tractor for raking total $41.33 per time, so the annual cost is calculated at $124. The labor cost is $16.53 in an eight-hour day, and manual raking time per unit area is 9.26 h/hm^2. The total proportion of time saved by OHRR compared to labor is 96.77%. According to Equations (16)-(18), the profitable area of OHRR is 6.7 hm^2. Since population aging in China nowadays has become more and more serious[33], with a large number of farmers now working in cities, the small-scale orchard farms have been replaced by large-scale modern fruit companies. Labor working is suitable for family farms, which have been eliminated in the industry. In such a circumstance, mechanized

OHRR is especially suitable for the large-scale mechanized orchard management. Orchard managers can use a certain amount of OHRR according to their orchard planting area and the cost that they can afford.

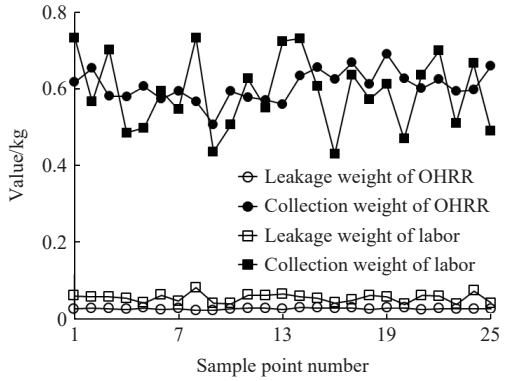

Figure 9 Leakage and collection weight of each sample point

Table 6 Strip density, width, height, and coefficient of variation (CV)

Test No.	Density/(kg·m^{-3})	CV/%	Width/m	CV/%	Height/m	CV/%
1	30.47	4.79	0.50	5.31	0.24	5.48
2	28.82	5.53	0.52	5.34	0.23	5.34
3	28.60	5.51	0.48	5.01	0.26	5.43
4	31.07	5.26	0.49	5.10	0.26	4.65
5	28.26	4.71	0.51	5.53	0.26	5.44
Average value	29.44	5.16	0.50	5.26	0.25	5.27

Table 7 Working efficiency and profitable area

Treatment	Working efficiency/(hm^2·h^{-1})	Profitable area/hm^2
OHRR	3.35	6.70
Labor	0.11	-

4 Conclusions

1) This study develops a small one-rotor orchard horizontal rotary rake (OHRR), which is used for grass collection in the mowing agronomic section of orchard management. OHRR is linked with a tractor by three-point suspension. The whole work process of the machine is completed by the hydraulic control system and mechanical transmission system of the tractor. In the working process, the disc drives the arms rotating around the vertical shaft, the guide cam that is fixed to the vertical shaft controls tine movement, and the tines turn to different inclination angles in different positions. The kinematic validation model of OHRR was built based on the theory that there is no gap or small overlap between the two adjacent working areas of the tines. This model determines the relationship between the advancing speed, disc rotational speed, rotation radius, arm number, and tine working width.

2) The leakage and repeating rates of OHRR virtual prototype were calculated by tine movement trajectory analysis in multi-body dynamics simulation. Box-Behnken three-factor and three-level test plans for advancing speed, disc rotational speed, and tine working width were designed to obtain the optimal operation parameters of the OHRR: advancing speed was 11.16 km/h, disc rotational speed was 6.98 rad/s, and tine working width was 0.3 m. Taking labor working as the control group, OHRR field tests were evaluated by four indices: strip density, leakage rate, working efficiency, and profitable area. Field test results showed that the leakage rate of OHRR was 4.56%, which meets the requirements of national standard JB/T10905. The strip density, width, and height of OHRR were 29.44 kg/m^3, 0.5 m, and 0.25 m, respectively. These data can provide support for the subsequent loading and transportation operation. The profitable area of OHRR was 6.7 hm^2, which is suitable for large-scale mechanized orchard management.

Acknowledgements

This work was supported by National Natural Science Foundation of China (Grant No. 32201680), China Agriculture Research System of MOF and MARA (Grant No. CARS-28-21), National Science and Technology Development Program of China (Grant No. NK2022160104), Jiangsu Agricultural Machinery Integrated Program (Grant No. JSYTH01), Nanjing Modern Agricultural Machinery Equipment and Demonstration Technology Innovation Project (Grant No. NJ[2024]01), and Jiangsu Modern Agricultural Machinery Equipment and Technology Demonstration Extension Fund (Grant No. NJ2024-24).

[References]

[1] Xiang Y Z, Li Y, Liu Y, Zhang S Y, Yue X J, Yao B, et al. Factors shaping soil organic carbon stocks in grass covered orchards across China: a meta-analysis. Science of the Total Environment, 2022; 807(2): 150632.

[2] Pausic A, Tojnko S, Lesnik M. Permanent, undisturbed, in-row living mulch: A realistic option to replace glyphosate-dominated chemical weed control in intensive pear orchards. Agriculture Ecosystems & Environment, 2021; 318: 107502.

[3] Mo M H, Liu Z, Yang J, Song Y J, Tu A G, Liao K T, et al. Water and sediment runoff and soil moisture response to grass cover in sloping citrus land, southern China. Soil and Water Research, 2019; 14(1): 10–21.

[4] Wu Y P, Wang X, Hu R G, Zhao J S, Jiang Y B. Responses of soil microbial traits to ground cover in citrus orchards in central china. Microorganisms, 2021; 9(12): 2507.

[5] Li X L, Chu Y N, Jia Y H, Yue H Y, Han Z H, Wang Y. Changes to bacterial communities and soil metabolites in an apple orchard as a legacy effect of different intercropping plants and soil management practices. Frontiers in Microbiology, 2022; 13: 956840.

[6] Lei X H, Qi Y N, Zeng J, Yuan Q C, Chang Y H, Lyu X L. Development of unilateral obstacle-avoiding mower for Y-trellis pear orchard. Int J Agric & Biol Eng, 2022; 15(1): 71–78.

[7] Bai G S, Zhou N, Shao F Q, Du J H, Guo J P. Effects of self-sown grass on soil nitrogen and apple fruit quality in the Weibei dry platean. Transactions of the CSAE, 2021; 37(10): 100–109.

[8] Duan Z L, Wang C G, Song Y. Effects of different green manure cultivation models on soil physical properties, apple quality and yield in fruit regions of Northern Shaanxi. China Fruits, 2022; 1: 24–28.

[9] Wang C W, Zhang N, Bao D S, Meng Y G, Zhang L. Comparative analysis of typical rake at home and abroad and development suggestions of domestic rake. Agricultural Engineering, 2021; 11(2): 6–11. (in Chinese)

[10] Yang L. Development status and tendency of rake swather. Journal of Agricultural Mechanization, 2020; 41(4): 57–64.

[11] Liu X H, Li J Y, Li B H. Design and test of 9LX-5.0 type double rotor horizontal rotating rake. Agricultural Development & Equipments, 2018; 1: 102–103. (in Chinese)

[12] Wang Z Y, Guo Z P, Wu W L, He Z Q. Fatigue life analysis of spring teeth of double rotor horizontal rotating rake. Journal of Agricultural Mechanization Research, 2022; 44(10): 14–18.

[13] Zhai G X, He G, Wang Q, Wang Z H, Yang L, Dong J J. Innovative design of ground profile mechanism of horizontal rotary rake. Farm Machinery, 2021(12): 64–68.

[14] Wang D C, He C B, Wu H J, You Y, Wang G H. Review of alfalfa full-mechanized production technology. Transactions of the CSAM, 2017; 48(8): 1–25.

[15] Paraforos D, Griepentrog H, Vougioukas S. Modeling and simulation of a four-rotor rake loading for predicting accumulated fatigue damage: a markov regime-switching approach. Applied Engineering in Agriculture, 2018; 34(2): 317–325.

[16] Abby E, Craig C, Daniel J, Marvin H, Daniel M, Krishona L, et al. Hay

rake-type effect on ash and forage nutritive values of alfalfa hay. Crop Economics, Production & Management, 2017; 109(5): 2163–2171.

[17] Khalid A. Impact of raking and baling patterns on alfalfa hay dry matter and quality losses. Saudi Journal of Biological Sciences, 2018(25): 1040–1048.

[18] National Development and Reform Commission, The rotary rake, 2008; JB/T 10905-2008. (in Chinese)

[19] Li T, Qiu Q, Zhao C J, Xie F. Task planning of multi-arm harvesting robots for high-density dwarf orchards. Transactions of the CSAE, 2021; 37(2): 1–10.

[20] Kang F, Tong S Y, Zhang H S, Li W B, Chen Z J, Zheng Y J. Analysis and experiments of reciprocating cutting parameters for apple tree branches. Transactions of the CSAE, 2020; 36(16): 9–16.

[21] Hu F J, Yang H B, Sheng Z L, Luo H Y, Zhai X M, et al. Research progress of weed control in tea garden. Journal of Henan Agricultural Sciences, 2018; 47(10): 7–11.

[22] Jiang H G, Zhang Y Z, Zhu X X, Li Y Y. A new barrier material for preventing weed proliferation in plantation of young tea bushes. Acta Tea Sinica, 2017; 58(4): 189–192. (in Chinese)

[23] Zhao X, Ma X X, Liao H W, Xiong Y S, Xu Y D, Chen J N. Design of flower transplanting mechanisms based on double planet carrier non-circular gear train with complete rotation kinematic pair. Int J Agric & Biol Eng, 2022; 15(3): 9–15.

[24] Zhou M L, Shan Y Y, Xue X L, Yin D Q. Theoretical analysis and development of a mechanism with punching device for transplanting potted vegetable seedlings. Int J Agric & Biol Eng, 2020; 13(4): 85–92.

[25] Zhao X, Zhang X S, Wu Q P, Dai L, Chen J N. Research and experiment of a novel flower transplanting device using hybrid-driven mechanism. Int J Agric & Biol Eng, 2020; 13(2): 92–100.

[26] Yu Z H, Huai S C, Wang W M. Leakage rate and optimization of working parameters for cylinder pickup collector based on spring-finger trajectory. Transactions of the CSAE, 2018; 34(4): 37–43.

[27] Xu H Z, Tian D Y, Liu J D, Niu Z H, Li Q. Operation analysis and parameter optimization of drum type soil-covering device. Int J Agric & Biol Eng, 2021; 14(3): 123–129.

[28] Hu H N, Li H W, Wang Q J, He J, Lu C Y, Wang Y B, et al. Anti-blocking performance of ultrahigh-pressure waterjet assisted furrow opener for no-till seeder. Int J Agric & Biol Eng, 2020; 13(2): 64–70.

[29] Zhai G X, Liu G L, He G, Bao D S, Wang Q X, Zhang P. Design and experiment on the horizontal rotary rake. Journal of Agricultural Mechanization Research, 2014; 36(7): 168–173.

[30] JB/T 9700-2013. Results of test methods for machines of hay harvesting. Ministry of Machine-Building Industry of the People's Republic of China, 2013. (in Chinese)

[31] GB/T 14247-2015. Rake testing methods. Inspection and Quarantine of the People's Republic of China (AQSIQ), 2015. (in Chinese)

[32] Lei X H, Lyu X L, Zhang M N, Lu D P, Wang S L, Chang Y H, et al. Performance evaluation of mechanical blossom thinning in trunk type pear orchard. Int J Agric & Biol Eng, 2021; 14(4): 106–112.

[33] Zheng Y J, Jiang S J, Chen B T, Lü H T, Wan C, Kang F. Review on technology and equipment of mechanization in hilly orchard. Transactions of the CSAM, 2020; 51(11): 1–20. (in Chinese)